DOI: 10.13009/EUCASS2017-124

Experimental investigation of plasma-assisted supersonic combustion

A. Vincent-Randonnier[1], D. Packan[1], V. Sabelnikov[1,2], F. Le Jouan[1], B. Rouxel[1], P. Roux[1], and S. Leonov[3]
[1]ONERA – The French Aerospace Laboratory, Palaiseau, F-91761, France
[2]Central Aerohydrodynamic Institute (TsAGI), 140180 Zhukovsky, Moscow Region, Russian Federation
[3]University of Notre Dame,Notre Dame, IN, 46556, USA

Abstract

This paper presents the first experiments performed at the LAERTE facility (ONERA – Palaiseau Center) with a plasma/injection module flush-mounted in the LAPCAT2 Dual Mode Scramjet combustor. Experiments were performed with Mach 2.0 nozzle at plenum stagnation temperature of dry air (T_0) of 270 K, plenum stagnation pressure (P_0) of 0.21 MPa, air mass flow rate ($\dot{m}_{air}$) of 405 g/s. A multi-electrode quasi-DC discharge was generated 20 mm upstream from the fuel injection ports. The experiments were performed without and with hydrogen injection (hydrogen H_2 mass flow rate $\dot{m}_{H2}$=1.0 g/s, fuel-air equivalence ratio ER=0.114). The behaviour of the discharge was strongly modified at the presence of the hydrogen injection (smaller discharge area than in pure air, plasma power of 1.5 kW instead of 7.4 kW). When plasma is generated in the hydrogen/air mixture, a significant pressure increase is observed along the combustor which is possibly due to supersonic combustion. With the same combustor without the plasma assistance, a total air temperature around 1500 K is necessary to reach hydrogen self-ignition conditions.

Nomenclature

DM	Dual-mode
h	specific enthalpy ($MJ\cdot kg^{-1}$)
HV	High Voltage
M	Mach number
$\dot{m}$	mass flow rate
P_0	Total pressure (stagnation conditions)
P_S	Static pressure
Quasi-DC	Quasi-Direct Current
PAC	Plasma Assisted Combustion
T_0	Total temperature (stagnation conditions)
T_S	Static temperature
YSZ	Yttria-Stabilized Zirconia (thermal barrier coating)

1. Introduction

Dual-mode (DM) ramjet/scramjet is the most promising air-breathing engine to propel future high-speed aircrafts/vehicles [1,2]. Typical ramjet range of use is 3≤ flight Mach number M≤5–5.5 with a flight level between 15 and 30 km. Ramjet and scramjet propulsion is studied at ONERA since the early 1950’ s [1-3]. In 2010, the LAERTE facility at ONERA–Palaiseau Center has been equipped with a DM ramjet/scramjet combustor, which was developed, manufactured and used within the LAPCAT2 project (EU 7th Framework Programme, 2008-2013) [6-8]. This project aimed at investigating hypersonic propulsion concepts for long haul passenger transport (flight Mach number M 6–8; altitude 18000 m).

In the supersonic combustion regime, several issues are encountered:

- difficulties of fuel-air mixing in supersonic flows;
- short residence time in the combustor combined with the slow kinetics of ignition at low/moderate temperature (at flight Mach number M=5–6);
- combustion instabilities.

These issues are responsible for the limitation in flight altitude. As plasma discharges enable to improve/stabilize combustion by their chemical, thermal and gas dynamical effects [9-14], they can enlarge the flight domain, especially at high altitude, as shown in Figure 1.

DOI: 10.13009/EUCASS2017-124

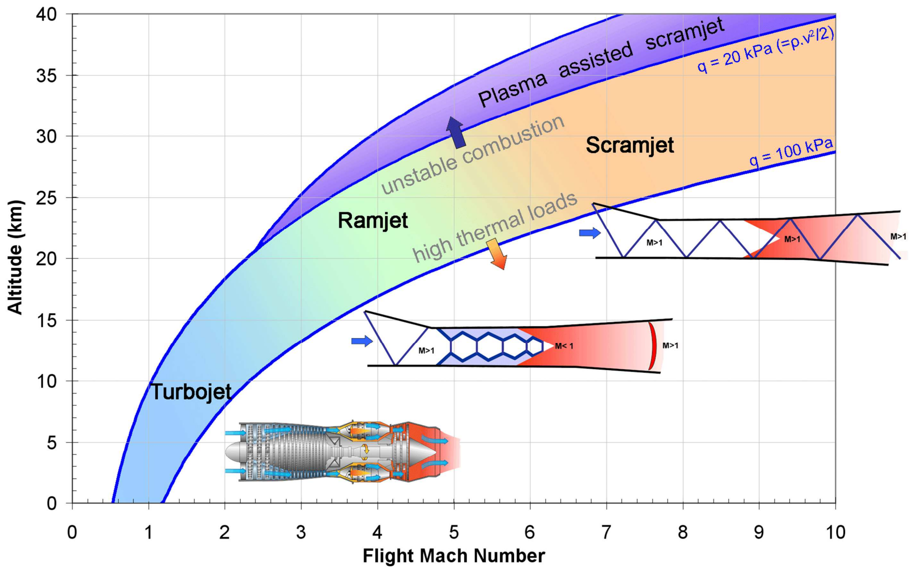

Figure 1: Flight domain for high speed propulsion

Recently, ONERA designed a module coupling plasma quasi-direct current (quasi-DC) discharge and fuel injection based on the concept proposed by Leonov et al. [15,16]. The current work focuses on the first experiments in plasma-assisted supersonic combustion using the LAPCAT2 DMScr combustor equipped with this plasma/injection module.

2. Experimental set-up

2.1 The LAERTE facility

One of the test lines of the LAERTE facility is used to feed the LAPCAT2 DM ramjet/scramjet combustor with hot vitiated-air (heating by H_2/air combustion and O_2 replenishment to maintain O_2 molar fraction to 0.21). It is operated in the connected pipe mode. Total temperature (T_0) and pressure (P_0) can reach up to 1800–1900K and 1.0–1.2MPa, respectively. They are measured in a pipe with an inner diameter of 105 mm at 220 mm upstream from the throat of the de Laval nozzle delivering the air mass flow rate at the entrance of the combustor. Even if pressure is measured at the wall, it is assumed to equal total pressure as the local Mach number is 0.054 (P/P_0=0.998).
Embedded instrumentation also includes the measurement of static pressure along the combustor, using up to 128 wall pressure transducers scanned at 10Hz. The sensors are calibrated before each test campaign, according to ONERA's quality procedures (ISO 9001 certification). A computer-based system controls the reproducibility and stability of the operating conditions.
The outlet of the combustor is connected to a 400 mm diameter exhaust pipe where the pressure is around 0.1 MPa (ambient pressure). Figure 2 presents a schematic of the facility.

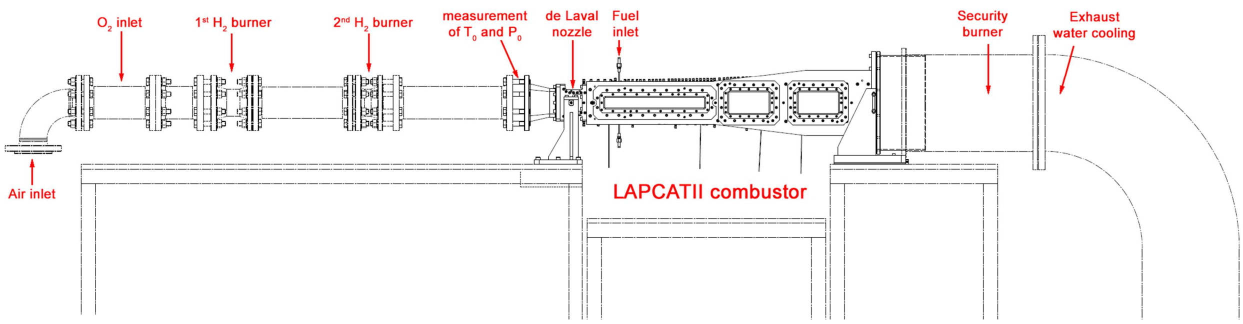

Figure 2: Schematic of the LAERTE facility

DOI: 10.13009/EUCASS2017-124

2.2 The LAPCAT2 combustor

The supersonic flow is generated by Mach M 2.0 (de Laval) nozzle, where the reference position (x=0 mm) corresponds to the throat. The combustor (Figure 3) consists of four sections: the first one (55 mm<x_1<280 mm) has a constant cross-section, the following sections (280 mm<x_2<598 mm<x_3<952 mm<x_4<1257 mm) have respectively 1°, 3° and 1° of diverging half angles to prevent/stunt thermal choking. The combustor width is constant (40 mm) and inlet height is 35.4 mm. Due to the 0.1MPa back pressure in the exhaust pipe, the combustor is over-expanded for total pressure below 0.9MPa: a boundary layer detachment occurs in the combustor at a position depending on the total pressure.
Large fused silica windows (seen in Figure 3) placed at the locations shown in Figure 4 allow visualization and optical diagnostics. The combustion chamber is made of a copper alloy. Inner walls are coated with a 0.3 mm thick YSZ (Yttria-Stabilized Zirconia) thermal barrier.
As the combustor is not water cooled, the overall duration of a test run is limited to around 1 minute but the useful duration, i.e. at required temperature, lasts between 5s and 15s, depending on test conditions.
The fuel used in the current study was pure gaseous hydrogen.

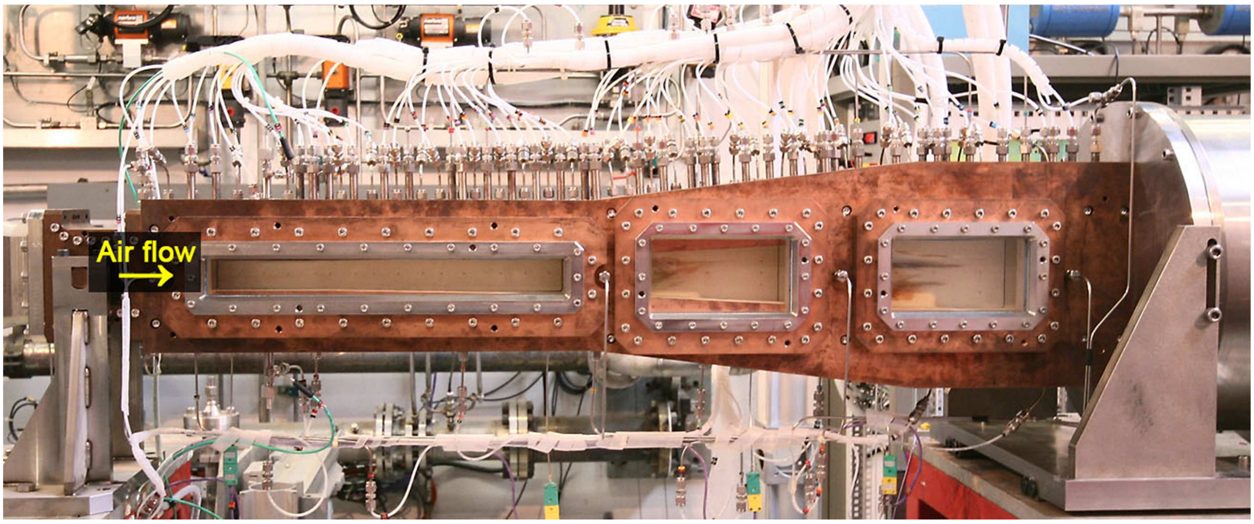

Figure 3: Side view of the combustor (without plasma module)

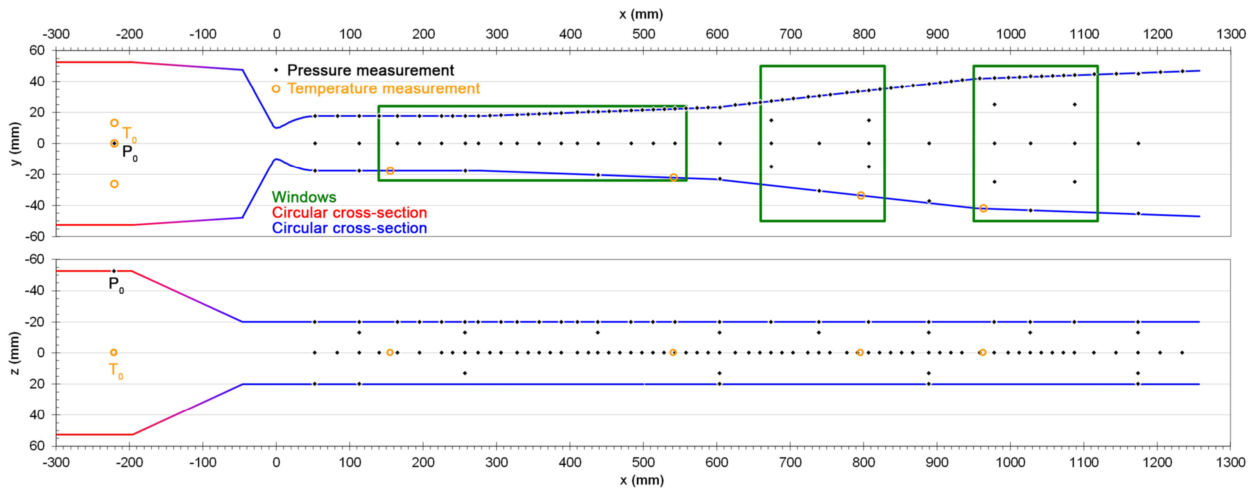

Figure 4: Geometry of the LAPCAT-II combustor showing the position of pressure ports and side windows

DOI: 10.13009/EUCASS2017-124

2.3 The plasma/injection module

The first tests on the Plasma-Assisted Combustion at the LAERTE facility were started in 2016. The design on the plasma/injection module and some results are presented below. The plasma/injection module was manufactured and assembled by Microcertec [17]. It is made of a cordierite glass ceramic (Corning 9606). It includes:

- a set of high voltage (HV) electrodes (at x=180 mm, x=226 mm and/or x=286 mm),
- fuel injectors (at x=200 mm and/or x=251 mm),
- two ground electrodes surrounding HV electrodes and fuel injectors.

The Figure 5 depicts the arrangement of the electrodes and fuel injection holes of this module. It is flush-mounted at the wall of the LAPCAT2 combustor, replacing the side window. The module was fed with hydrogen which was injected with a sonic velocity through two 2 mm diameter cylindrical ports located at x=200 mm (side wall) whereas electrical power was only applied to the upstream HV electrode (at x=180 mm). The shortest gap between HV and ground electrodes is 4 mm.

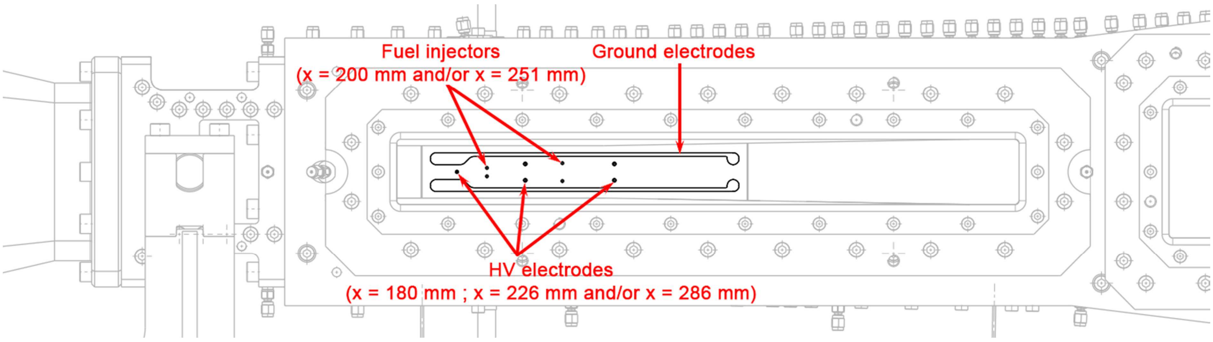

Figure 5: Schematic of the plasma/injection module

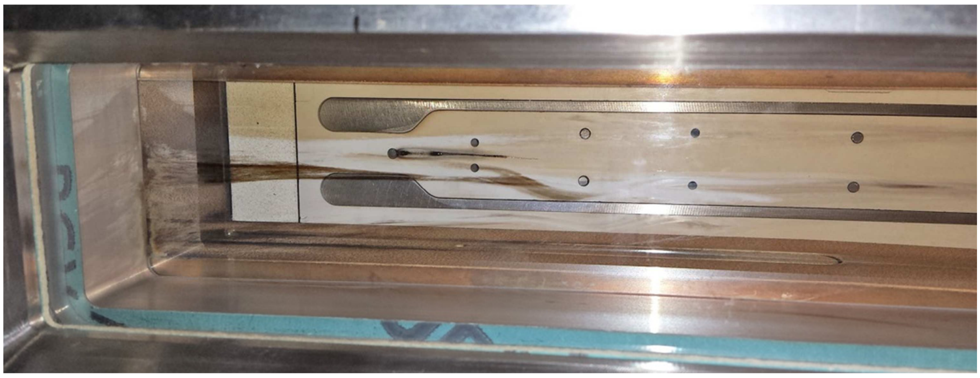

Figure 6: Plasma/injection module connected to the supersonic combustor

2.4 Power supply and electrical measurements methodology

The plasma discharge was produced using a 5 kV–3.4 A DC power supply in the current regulation mode. A 300 Ω ballast resistor was used to stabilize the discharge. A high voltage probe Tektronix P6015A (1000:1 attenuation) was used to measure the voltage applied to the HV electrode (U1 in Figure 7). A second HV probe, a Lecroy PPE20kV (U2 in Figure 7), was used to estimate the potential drop at the resistor, thus allowing to calculate the current $I(t)$. A fast digital oscilloscope LeCroy 6050 (band width 1 GHz, 4 channels, 12.5 Msamples/channel) acquired both voltage signals. Digitized electrical signals were stored and processed to estimate instantaneous and averaged electrical power. The high voltage was applied to the plasma generator during about 1 second.

In static air at ambient conditions (T=300 K, P=0.1MPa, density ≈ $2.4\cdot 10^{19}$ cm^{-3}), and according to Paschen's law [18,19] (discharge generated in the gas between two parallel-plate electrodes), the breakdown voltage is around 16 kV DC for a gap of 4 mm. In the present study, as the plasma module generates surface discharges in a non-uniform electric fields due to the electrodes geometry, the breakdown voltage should be slightly lower but remains

DOI: 10.13009/EUCASS2017-124

unattainable with a 5kV DC generator. With a Mach 2.0 supersonic air flow at P_0=0.21MPa, the static pressure drops to P_S≈0.037MPa in the combustor (at *x*=200mm) thus reducing the breakdown voltage down to around 5 kV, making it possible to reach breakdown conditions.

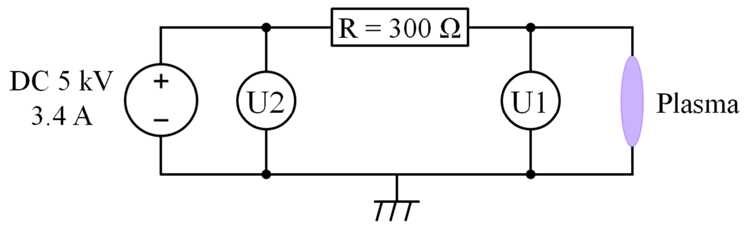

Figure 7: Principal layout of electrical circuit

3. Results and discussion

As shown in a previous study [7], with the same combustor without plasma assistance, air should be heated up to T_0≈1500K (T_S≈960K) to initiate supersonic combustion (P_0=0.40 MPa) and produce a significant heat release. In the current study, tests of plasma-assisted combustion have been carried out in cold supersonic dry air flow (M=2.0; T_0=270K, P_0=0.21MPa, $\dot{m}_{air}$=405g·s^{-1}). The combustor is then over-expanded and the boundary layer detachment occurs around *x*=450–500mm (recovery of the outlet pressure level), as indicated in Figure 8.

3.1 Non-reacting case

When high voltage is applied to electrode in air without fuel injection, the plasma discharge induces a small pressure increase in the combustor. As the pressure measurement is accurate enough to exclude measurement uncertainties (30–40kPa±90Pa), this increase is presumably due to the heat release by the discharge. Indeed, according to Leonov et al. [20,21], the power dissipated in the plasma filament results in significant local temperature increase (T=3000K ±500 K) in the case of a quasi-DC near-surface discharge in a supersonic air flow.

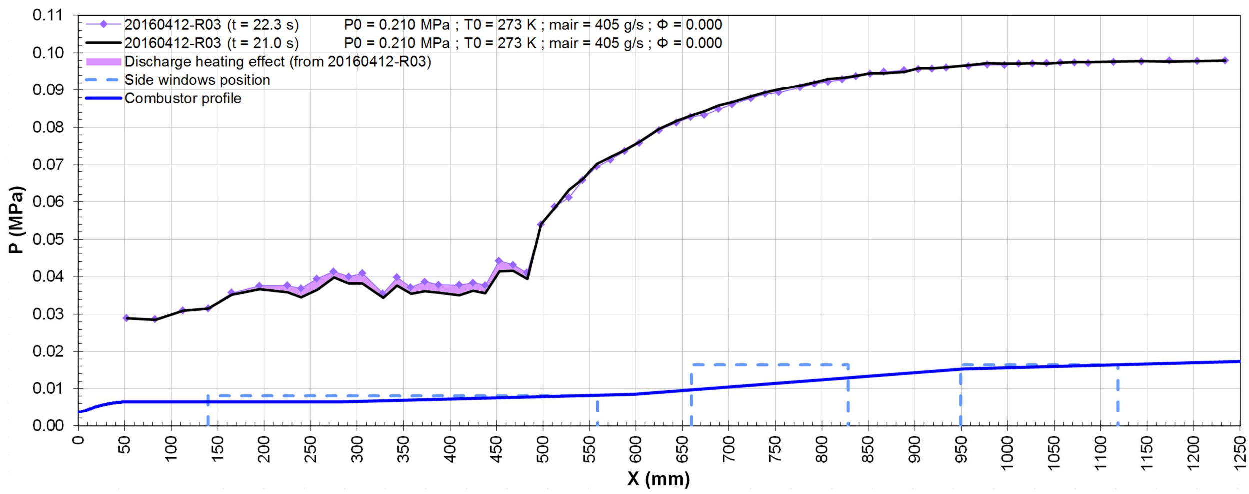

Figure 8: Effect of the plasma discharge on the pressure profile (—●— air flow ; —●— air flow + discharge

The Figure 9 presents an image of the discharge in the cold supersonic air flow without fuel injection. It has been extracted from movies recorded with a full-HD camcorder operating at 25 fps. It is consequently time-integrated which prevents the visualization of individual plasma filaments. The purple emission is a usual feature of discharges in air (second positive system of nitrogen). It is visible up to 130 mm downstream of the HV electrode.
The filamentary discharge is initiated at the shortest interelectrode distance (4 mm) and then blown away and cooled down by the flow up to its extinction. Then a new discharge is initiated. Based on electrical measurements, the average duration of the filament expansion/convection is about 650 µs. Breakdown occurs for a voltage around 4.7 kV whereas average current and voltage are 7.1 A and 1.0 kV respectively.

DOI: 10.13009/EUCASS2017-124

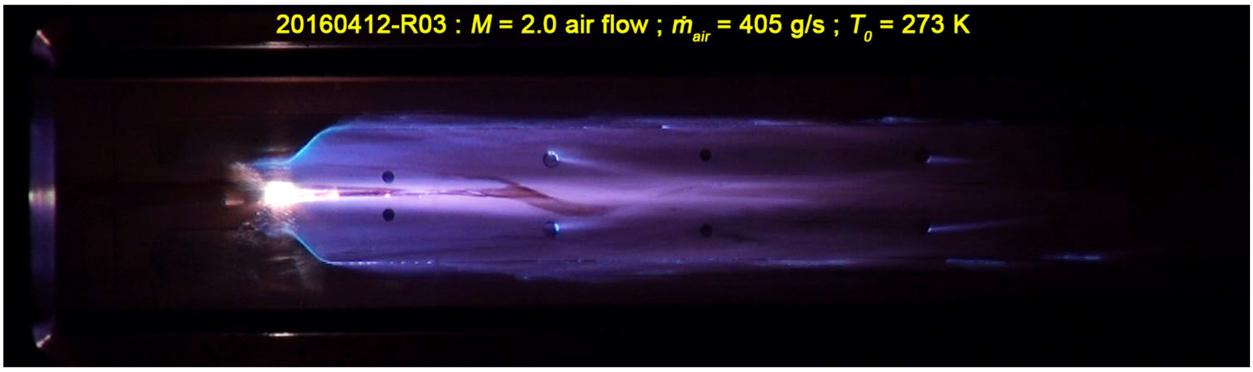

Figure 9: Discharge in a cold Mach 2 air flow without fuel injection

3.2 Reacting case

When hydrogen is injected in the supersonic air cross-flow (M=2.0; T_0=270K, P_0=0.21MPa, $\dot{m}_{air}$=405 $g\cdot s^{-1}$, $\dot{m}_{H2}$=1.0 $g\cdot s^{-1}$, ER=0.114) with the discharge off, a bow shock is generated and the boundary layer detaches upstream from the fuel jet [7,22,23] thus leading to a pressure increase (red line in Figure 10).

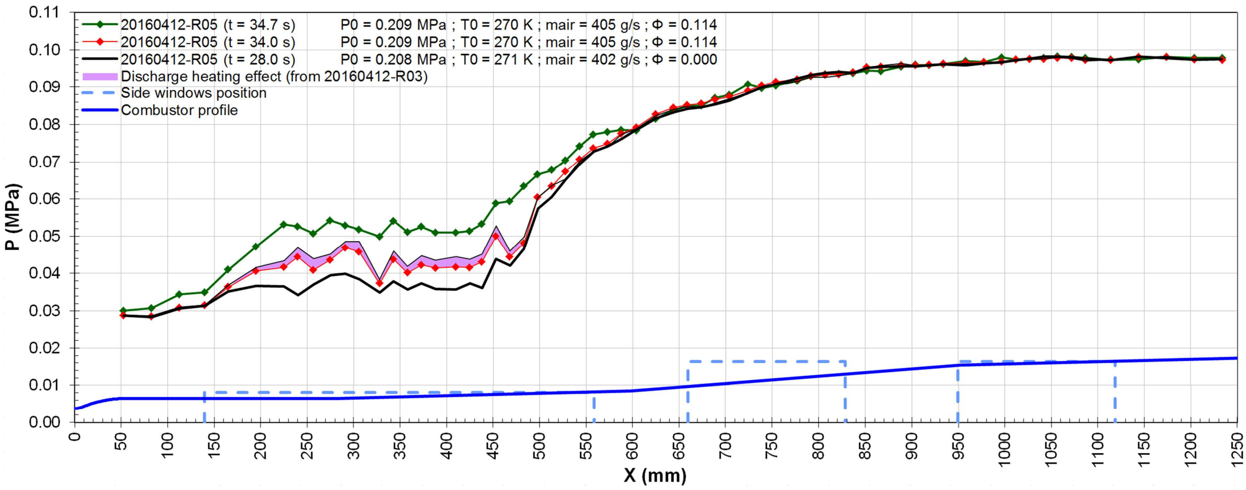

Figure 10: Effect fuel injection and plasma discharge on the pressure profile (—●— air flow ; —●— air flow + H_2 injection ; —●— air flow + H_2 injection + discharge)

As the momentum ratio between the hydrogen jets and the incoming air flow is low ($\approx 6\cdot 10^{-3}$), the induced recirculation zones and separated regions presumably remain small.

If the HV generator is switched on with the same settings than for the non-reacting case, the discharge is generated but its area is significantly smaller than in pure air (40–50 mm long instead of 130 mm), as shown in Figure 11. The electrical properties of the discharge in the air + hydrogen mixture are strongly modified as well: the average duration of the filament expansion/convection can reach several ms, breakdown occurs at a slightly lower voltage (around 4.3 kV) and the average current and voltage are 5.4A and 0.3kV respectively. At the same time, the pressure profile in the combustor significantly increases (green line in Figure 10; x<600mm). Different effects can contribute to this pressure increase:

- the gas heating by the discharge,
- the gas heating due to the subsonic combustion of the fuel in a recirculation area or in the detached boundary layer,
- the gas heating due to supersonic combustion,
- the reinforcement by the discharge of the fuel injection shock/boundary layer detachment.

As the plasma power (around 1.5kW) corresponds to less than 1% of the air flow enthalpy (specific enthalpy h=0.27$MJ\cdot kg^{-1}$), the contribution of the heat release by the discharge to the pressure increase is assumed to be small. By comparison, the purple area in Figure 10 depicts the pressure increase due to the discharge in pure air with a significantly higher plasma power (7.4kW).

DOI: 10.13009/EUCASS2017-124

The presence of a clearly visible pink emission in the wake of the injection holes (Figure 11) is likely due to the combination of the Balmer emission lines of atomic hydrogen (H_α at 656.3 nm and H_β at 486.1 nm). These emission lines have been identified by Firsov et al. [24] in Quasi-DC discharges. Atomic hydrogen is highly reactive specie and an efficient promoter of combustion. Anyway, complementary measurements such as Schlieren and/or OH^* radical imaging, temperature and composition measurement of the burnt gas in the combustor are mandatory to quantitatively determine the contribution of each effect to the pressure increase.

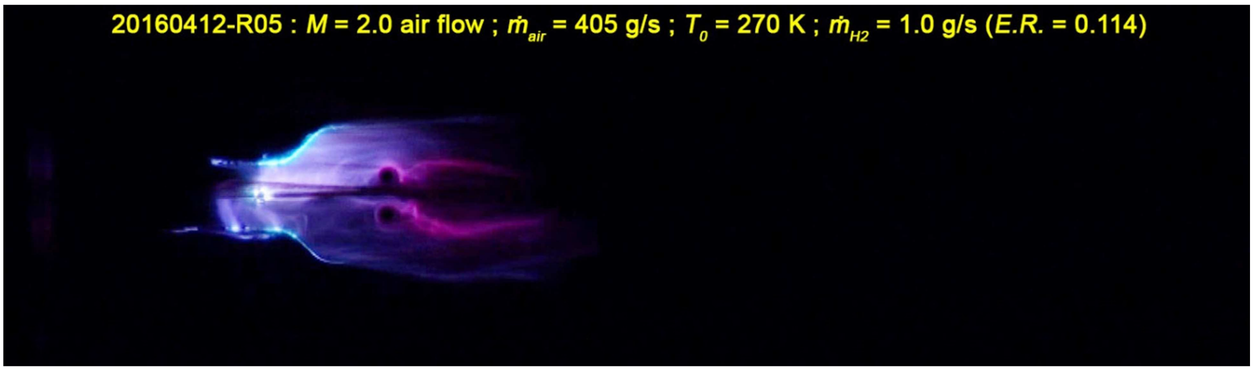

Figure 11: Discharge in a cold Mach 2 air flow with H2 injection

4. Conclusions

A module coupling fuel injection and generation of plasma discharges has been designed and manufactured to be flush-mounted in the LAPCAT2 Dual Mode Scramjet combustor at ONERA Palaiseau Center. Quasi-DC discharges were generated 20 mm upstream from the fuel injection ports in a cold supersonic air flow (M=2.0; T_0=270 K, P_0=0.21 MPa, $\dot{m}_{air}$=405 g/s). When hydrogen is injected ($\dot{m}_{H2}$=1.0 g/s, ER=0.114), significant pressure increase was observed in the combustor, the average plasma power being around 1.5 kW which corresponds to less than 1% to the air flow enthalpy. This pressure increase is possibly due to the heat release by the combustion of hydrogen, to the gas heating by the discharges and/or to the modification by the discharges of the flow pattern arising from transverse injection (reinforcement of the bow shock, the detachment area…).
These preliminary results validate the design of the module and the relevance of the selected approach. They will be complemented in the oncoming months by the OH* radical imaging to confirm combustion and the detailed study of the electrical properties of the discharge. Along with the plasma assisted combustion experiments, the dynamics of the discharge filaments will be characterized using high-speed visualization and spectroscopic measurements will be used to determine their temperature.

Acknowledgments

Authors would like to thank A. Merlen and L. Jacquin, Directors of Energetics Branch of ONERA, for the financial support to plasma assisted supersonic combustion experiments. V. Sabelnikov was also partially supported by the Grant of the Ministry of Education and Science of the Russian Federation (Contract No. 14.G39.31.0001 of 13.02.2017) during the analysis of the experimental data.

References

[1] Smart, M., "Scramjets," Advances on Propulsion Technology for High-Speed Aircraft, NATO Science and Technology Organization – RTO-EN-AZVT-150 (2007)

[2] Bouchez, M., "Statoréacteur - Propulsion aérobie moyenne ou grande vitesse," Techniques de l'ingénieur – BM-3-020 (2012)

[3] http://www.onera.fr/en/history/onera-70-years-1946-1962-aeronautical-research-that-is-rapidly-gaining-momentum

[4] Le Pichon T., Laverdant A., Numerical Simulation of Reactive Flows in Ramjet Type Combustors and Associated Validation Experiments, AerospaceLab Journal, Issue 11 (2016), DOI: 10.12762/2016.AL11-03 (http://www.aerospacelab-journal.org/sites/www.aerospacelab-journal.org/files/AL11-03.pdf)

DOI: 10.13009/EUCASS2017-124

[5] Scherrer D., Dessornes O., Ferrier M., Vincent-Randonnier A., Sabel'nikov V., Moule Y., “Research on supersonic combustion and scramjet combustors at ONERA”, AerospaceLab Journal, Issue 11 (2016), DOI: 10.12762/2016.AL11-04 (http://www.aerospacelab-journal.org/sites/www.aerospacelab-journal.org/files/AL11-04.pdf)

[6] Steelant J., Varvill R., Defoort S., Hannemann K., Marini M., “Achievements Obtained for Sustained Hypersonic Flight within the LAPCAT-II Project”, *20th AIAA International Space Planes and Hypersonic Systems and Technologies Conference*, Glasgow (Scotland – UK), 2015, AIAA 2015-3677

[7] Vincent-Randonnier A., Moule Y., Ferrier M., Combustion of hydrogen in hot air flows within LAPCAT–II Dual Mode Ramjet combustor at Onera-LAERTE facility – Experimental and Numerical Investigation, 19th AIAA International Space Planes and Hypersonic Systems and Technologies Conference, Atlanta (GA), 2014, AIAA 2014–2932

[8] Defoort S., Ferrier M., Serre L., Scherrer D., Paridaens C., Hendrick P., Ingenito A., Bruno C., LAPCAT-II : Conceptual design of a Mach 8 TBCC civil aircraft, enforced by full Navier-Stokes 3D nose-to-tail computation, 17th AIAA International Space Planes and Hypersonic Systems and Technologies Conference, San Francisco (CA), 2011, AIAA 2011–2317

[9] Vincent-Randonnier A., Combustion enhancement and stabilization: principles of plasma assistance and diagnostics tools, Handbook of Combustion Vol. 5 (New Technologies) - Chapter 6, Wiley VCH publisher, 2010

[10] Starikovskaia S.M., Plasma assisted ignition and combustion, J. Phys.D: Applied Physics, 39 (2006) R265-R299

[11] Jacobsen L. et al., Plasma-assisted ignition in scramjets, J. Propul. Power, 24 (4) (2008) 641–654

[12] Takita K., Shishido K., Kurumada K., Ignition in a supersonic flow by a plasma jet of mixed feedstock including CH_4, Proc. Combust. Inst. 33 (2) (2011) 2383–2389

[13] Li F., Yua X-L., Tong Y-G., Shen Y., Chen J., Chen L-H. and Chang X-Y., Plasma-assisted ignition for a kerosene fueled scramjet at Mach 1.8. Aerospace Science and Technology 28 (2013) 72–78

[14] Poggie J., McLaughlin T. and Leonov S., Plasma aerodynamics: Current Status and Future Directions, Issue 10 (2015), DOI: 10.12762/2015.AL10-01 (http://www.aerospacelab-journal.org/sites/www.aerospacelab-journal.org/files/AL10-01.pdf)

[15] Leonov S. and Yarantsev D., “Plasma induced ignition and plasma-assisted combustion in high-speed flow”, Plasma Sources Science and Technology, 16 (2007) 132-138

[16] Leonov S., Vincent-Randonnier A., Sabelnikov V., Firsov A., Yarantsev D., Two-Stage Mechanism of Electrically Driven Combustion in Supersonic Flow, 21th Internation Symposium on Air-Breathing Engines, Busan (Korea), 2013, ISABE 2013-1630

[17] http://www.microcertec.com/

[18] Paschen F., Ueber die zum Funkenübergang in Luft, Wasserstoff und Kohlensäure bei verschiedenen Drucken erforderliche Potentialdifferenz, Analen der physic 273 (1889) 69-96

[19] Lieberman M. A. and Lichtenberg A. J., Principles of Plasma Discharges and Material processing (second edition), 2005, Wiley ed., ISBN 0-471-72001-1

[20] Leonov S., Adamovich I. and Soloviev V., Dynamics of near-surface electric discharges and mechanisms of their interaction with the airflow, Plasma Sources Sci. Technol. 25 (2016) 063001

[21] Savelkin K., Yarantsev D. and Leonov S., Experiments on Plasma-Assisted Combustion in a Supersonic Flow: Optimization of Plasma Position in Relation to the Fuel Injector, AerospaceLab Journal, Issue 10 (2015), DOI: 10.12762/2015.AL10-08 (http://www.aerospacelab-journal.org/sites/www.aerospacelab-journal.org/files/AL10-08.pdf)

[22] Ben Yakar A., Mungal M.G. and Hanson R.K., Time evolution and mixing characteristics of hydrogen and ethylene transverse jets in supersonic crossflows, Physics of Fluids 18 (2006) 026101

[23] Rana Z.A., Thornber B. and Drikakis D., Transverse jet injection into a supersonic turbulent cross-flow, Physics of Fluids 23 (2011) 046103

[24] Firsov A., Savelkin K., Yarantsev D. and Leonov S., Plasma-enhanced mixing and flameholding in supersonic flow, Phil. Trans. R. Soc. A 373 (2015) 20140337 (http://dx.doi.org/10.1098/rsta.2014.0337)